We are IntechOpen,
the world's leading publisher of Open Access books
Built by scientists, for scientists

6,900
Open access books available

186,000
International authors and editors

200M
Downloads

154
Countries delivered to

Our authors are among the

TOP 1%
most cited scientists

12.2%
Contributors from top 500 universities

CLARIVATE ANALYTICS

BOOK CITATION INDEX

INDEXED

WEB OF SCIENCE™

Selection of our books indexed in the Book Citation Index
in Web of Science™ Core Collection (BKCI)

Interested in publishing with us?
Contact book.department@intechopen.com

Numbers displayed above are based on latest data collected.
For more information visit www.intechopen.com

Synthetic Jet-based Hybrid Heat Sink for Electronic Cooling

Tilak T Chandratilleke, D Jagannatha and R Narayanaswamy
Curtin University
Australia

1. Introduction

Modern lifestyle is increasingly dependant on a myriad of microelectronic devices such as televisions, computers, mobile phones and navigation systems. When operating, these devices produce significant levels of internal heat that needs to be readily dissipated to the ambient to prevent excessive temperatures and resulting thermal failure. With inadequate cooling, internal heat builds up within electronic packages to raise microchip temperatures above permitted thermal thresholds causing irreparable damage to semiconductor material. Devices would then develop unreliable operation or undergo complete thermal breakdown from overheating with reduced working life. In electronic industry, 55 percent of failures are attributed to overheating of internal components. Therefore, effective dissipation of internally generated heat has always been a major technical consideration for microelectronic circuitry design in preventing overheating and subsequent device failure.

In recent years, the modern microelectronic industry has shown a dramatic growth in microprocessor operating power, circuit component density and functional complexity across the whole spectrum of electronic devices from small handheld units to powerful microprocessors, as evidenced by Figs. 1 and 2.
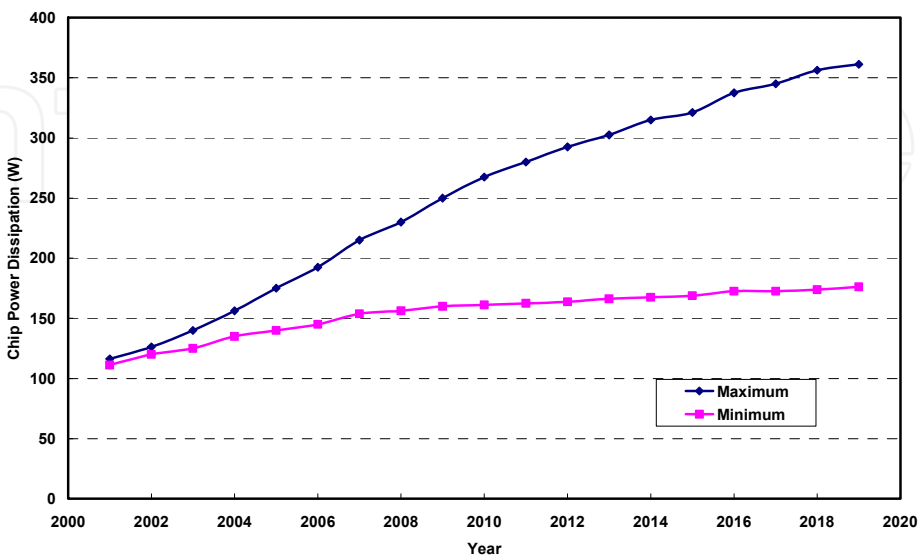

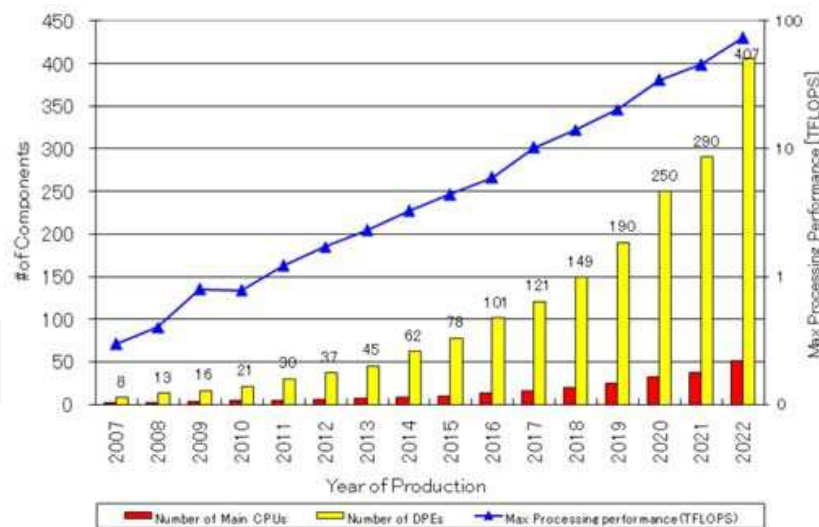Fig. 1. Evolution of chip power dissipation (Chu, 2003)

Fig. 2. Component density and maximum processing performance trends
Source: International Technology Roadmap for Semiconductors (ITRS)-2008

These industry trends into the future are very much poised to increase the microprocessor internal heat loads well beyond the capabilities of established cooling technologies making them rapidly inadequate to meet the predicted intense heat dissipation demand. For this, the future of electronic product design and development is critically hinged upon the availability of more enhanced or effective heat dissipation methods. This chapter presents a novel electronic cooling technique to address this current technological shortfall.

1.1 Thermal management techniques

In electronic system design, thermal management involves the use of appropriate heat transfer technology to remove internally generated heat as effectively as possible to retain component temperatures within safe operating limits. Literature identifies two specific stages for thermal management process. The first stage considers heat conduction from integrated circuit and to the encased package surface while the second stage deals with the global rejection of heat from the system to the ambient. Thus, the thermal management technologies can be broadly divided into two groups: (a) Technologies for enhancing heat flow integrated circuits to package surfaces, such as thermoelectric devices and heat pipes; (b) Technologies for enhancing heat exchange between the electronic package and the ambient, such as heat sinks, microchannels and fluid jet cooling. The work entailed in this chapter contributes to the latter group.

Thermal management techniques can be passive or active mechanisms. Passive techniques (e.g. convective heat sink, heat pipe) do not require additional energy input for operation; however their poor heat transfer capabilities overshadow this advantage. Intrinsically, active techniques (e.g. micro-refrigerator, microchannel heat sink) have better thermal performance, but are discredited by the extra operating power needs or higher pressure drop penalties. In spite of these limitations, active heat sinks firmly remain the most thermally effective and preferred option for future high-powered microcircuitry cooling applications, whilst passive heat sinks are being confined to low heat loads.

As an active thermal management technique, heat sinks utilising micro or mini fluid passages are highly regarded by the electronic industry to be the current frontier technology for meeting high heat dissipation demand. It has been estimated (Palm, 2001) that the

industry application of microchannel heat sinks would increase by 10 fold within the next 5 years in view of its high cooling potential achievable. A major drawback of microchannel heat sinks is their inherently high pressure drop characteristics, particularly at increased fluid flow rates necessary to deliver large cooling loads.

Motivated by the application needs of the electronic industry, the research on microchannel thermal behaviour has extensively progressed through numerical modelling and experimentation (Lee et al., 2005; Qu & Mudawar, 2002; Lee & Garimella, 2006). The primary focus of such research has been to predict and validate thermal performance. Much less attention has been directed for developing effective thermal enhancement strategies for micro-scale channels. The use of internal fins in microchannels has been identified to be a very promising passive enhancement option for single phase mini and microchannels (Steinke & Kandlikar, 2004) although the increased pressure drop is a design concern. This is well supported by a comprehensive treatment on such internal fins and possibilities for thermal optimisation (Narayanaswamy et al., 2008).

Whilst passive enhancement techniques have conceivable application potential, active methods are known to be more thermally effective and relevant for future cooling needs. Active heat sink systems can be made a more attractive proposition if an innovative approach could reduce operating power or pressure penalties without impacting on thermal performance. A hybrid heat sink incorporating a pulsating fluid jet offers a unique thermal enhancement option of this nature, as discussed below.

The proposed method utilises a special pulsing fluid jet mechanism called synthetic jet for enhancing convective heat transfer process in fluid flow channels of an active heat sink. This arrangement operates with unprecedented thermal performance but without the need for additional fluid circuits or incurring pressure drop, which are key features that set it apart from other traditional methods.

1.2 Synthetic (pulsed) jet mechanism and its behaviour

A synthetic jet is created when a fluid is periodically forced back and forth through a submerged orifice in such a way that the net mass discharged through the orifice is zero while generating large positive momentum in the jet fluid stream. A simple synthetic jet actuator is schematically shown in Fig. 3.
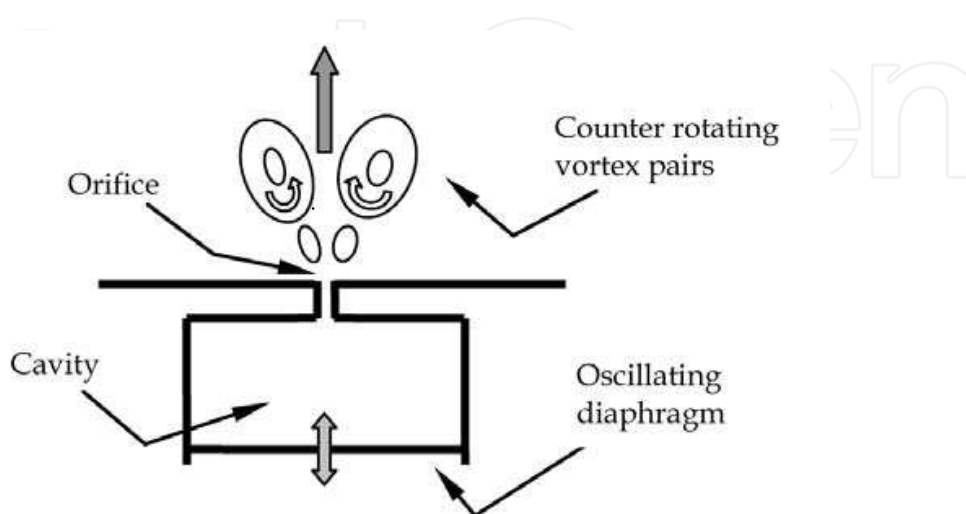

Fig. 3. Schematic diagram of a synthetic jet actuator

The actuator comprises of an oscillating diaphragm that resides within a cavity and induces a periodic fluid flow through a submerged orifice. In its upward motion, the diaphragm forces the fluid to be squirted out through the orifice with very large momentum. During downward motion, the diaphragm draws low-momentum fluid from the surroundings back into the cavity. Thus, over an operating cycle, the jet delivers very high net outflow of fluid momentum with no net change of fluid mass within the cavity. Owing to this unique feature, this jet flow is known as a synthetic jet or Zero-Net-Mass-Flux (ZNMF) jet (Smith & Glezer, 1998).

A synthetic jet impinging on a heated surface is capable of generating very high localised cooling because of the large fluid momentum imparted. As evident, this mechanism does not require additional fluid circuits to operate or introduce extra pressure drop to the flow field, which are major technical advantages. Synthetic jets are formed from the same working fluid in which they are deployed. This has significant benefits for microelectronic circuitry where air-cooling is preferred to prevent possible electrical short-circuiting and leakage faults. Smaller synthetic jet size permits high-flux clustered cooling without the need for fluid circulatory circuits unlike steady jets thereby reducing energy consumption and production cost. The diaphragm motion is practically achieved by a piston or acoustic loudspeaker or piezo-electric unit to obtain the desired amplitude or frequency.

Synthetic jets have been primarily studied in the context of pulsating jet actuators impinging on submerged surfaces in quiescent fluid media without any cross flow interactions. Such studies indicate outstanding thermal characteristics for localised cooling with synthetic jets. Significant examples of those are by (Campbell et al., 1998) who have demonstrated that synthetic air micro jets were effective cooling arrangements for laptop processors. (Mahalingam & Rumigny, 2004) illustrated the effectiveness of synthetic jets for high power electronic cooling by developing an integrated active heat sink based on this mechanism. (Gillespie et al., 2006) provide the results of an experimental investigation of a rectangular synthetic jet impinging on a unconfined heated plate exposed to the ambient where characteristics of the jet and plots of Nusselt numbers are available. (Pavlova & Amitay, 2006) have conducted experimental studies on impinging synthetic jets for constant heat flux surface cooling and compared its performance with a steady or continuous jet where there are no velocity fluctuations. They concluded that for the same Reynolds number, synthetic jets are three times more effective than the corresponding continuous jets.

(Utturkar et al., 2008) experimentally studied synthetic jet acting parallel to the flow within a duct. The synthetic jet was placed at the surface of a heated duct wall and aligned with the bulk flow such that the jet assisted the bulk flow. In a 100 mm square channel with a 30 mm synthetic jet, they obtained a 5.5 times enhancement for a bulk flow velocity 1 m/s. This enhancement reduced to approximately 3 times when the bulk velocity was increased to 2.0 m/s. Their numerical simulation matched reasonably well with only one test condition.

(Go & Mongia, 2008) experimentally studied the effect of introducing a synthetic jet into a low speed duct flow to emulate the confined flow within in a typical notebook. The interaction of these two flows was studied using particle image velocimetry (PIV) and measurements on the heated duct wall. They found that the synthetic jet tends to retard or block the duct flow while a 25 percent increase in thermal performance was observed.

Numerical studies on thermal performance of synthetic jet with cross flow interaction are also very limited in published literature. Such significant work is presented by (Timchenko et al., 2004) who investigated the use of a synthetic jet induced by a vibrating diaphragm to enhance the heat transfer in a 200 µm microchannel. Their two-dimensional (2-D) transient

simulation considered the jet acting in cross-flow to the bulk flow in a channel with the diaphragm executing a parabolic motion. They observed a 64 percent improvement in cooling at the impinging wall for the flow conditions used. Despite the recognised significance of flow turbulence in synthetic jet flows, their analysis however did not include an appropriate turbulence model in the simulation.

In a recent study, (Erbas & Baysal, 2009) conducted computational work of a synthetic jet actuator in a two-dimensional channel to assess its thermal effectiveness on a heated surface protruding into the fluid as a step. They varied the number of actuators, placement and phasing of the membrane concluding that the heat transfer rate would increase with the number of jets, appropriate jet spacing, the use of nozzle-type orifice geometry and 180º out of phase jet operation. However, the investigation did not examine the influence of cross flow on the thermal performance.

Performing a detailed parametric study, the work presented in this chapter evaluates and quantifies the thermal enhancement benefits for fluid flow through an electronic heat sink from a synthetic jet actuator mechanism. This hybrid arrangement is numerically simulated to obtain heat and fluid flow characteristics from which unique behaviour of the jet and cross-flow interaction is analysed. The degree of thermal enhancement is with respect to a heat sink unassisted by synthetic jet flow.

2. Synthetic jet hybrid heat sink - numerical model development

2.1 Geometrical description and operation

The present study proposes a hybrid arrangement for electronic cooling utilising a synthetic jet intercating with conventional fluid stream in heat sink, as depicted in Fig. 4. The synthetic jet is induced by a cavity fitted with an oscillating diaphragm that is mounted on the heat sink. The oscilatory motion of the diaphragm injects a pulsating fluid jet through a small orifice into the fluid stream in the heat sink's flow passage. The diaphragm moving inwards, ejects a high-speed jet that creating a pair of counter-rotating vortices in the surrounding fluid. When retreating, the diaphragm draws fluid back into the cavity. The
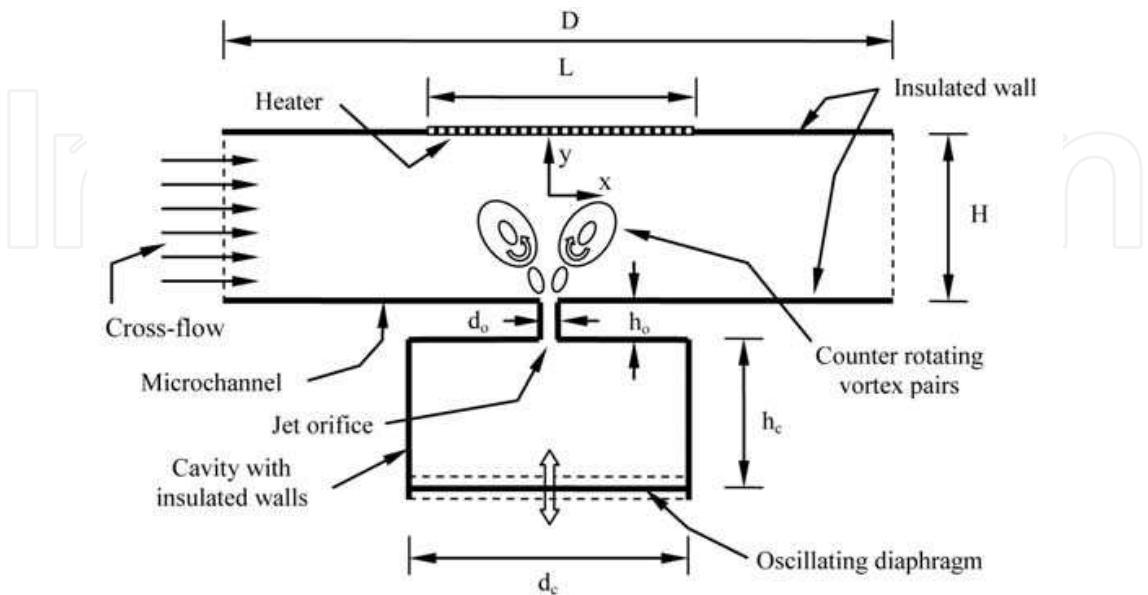

Fig. 4. Schematic diagram of synthetic jet mounted on heat sink in cross-flow configuration

fluid jet and its vortices interact in cross-flow manner with the fluid stream in heat sink's flow passage and perform periodic impingement on the heated wall. The operation over one diaphragm cycle is such, the jet delivers an intense momentum fluid outflow with zero net mass output through the orifice, hence complying with "synthetic jet" or Zero-Net-Mass-Flux jet condition.

The vortex formation associated with synthetic jet is governed by the non-dimensional groups Reynolds number (Re) and Stokes number (S), and occurs under the parametric condition of $Re/S^2 > K$, where the constant $K \approx 1$ for two-dimensional jets and 0.16 for axi-symmetric synthetic jets (Holman et al., 2005). Through due consideration of this requirement, the geometrical dimensions were selected for the 2-dimensional analytical model attempted. They are: orifice width $d_o = 50$ μm, orifice length $h_o = 50$ μm, channel height $H = 500$ μm, channel length $D = 2250$ μm, heater length $L = 750$ μm, cavity width $d_c = 750$ μm and cavity height $h_c = 500$ μm. This selection was checked for its compliance with the continuum mechanics for the scale of the attempted problem using Knudsen number Kn, which is the ratio of the molecular free path length to representative length.

2.2 Governing equations

This study investigates the heat transfer characteristics of low Reynolds number turbulent synthetic jets operating in a confined region while interacting with fluid flow in heat sink. Applicable governing equations for the analysis are: the Navier-Stokes equations; the continuity equation and the energy equation subject to applied boundary conditions. Air is assumed to be an incompressible Newtonian fluid although compressibility effects are considered later. These equations are as follows:

Continuity
$$\frac{\partial u}{\partial x} + \frac{\partial v}{\partial y} = 0 \tag{1}$$

x-momentum
$$\frac{\partial u}{\partial t} + u\frac{\partial u}{\partial x} + v\frac{\partial u}{\partial y} = -\frac{\partial p}{\partial x} + \mu\left(\frac{\partial^2 u}{\partial x^2} + \frac{\partial^2 u}{\partial y^2}\right) \tag{2}$$

y-momentum
$$\frac{\partial v}{\partial t} + u\frac{\partial v}{\partial x} + v\frac{\partial v}{\partial y} = -\frac{\partial p}{\partial y} + \mu\left(\frac{\partial^2 v}{\partial x^2} + \frac{\partial^2 v}{\partial y^2}\right) \tag{3}$$

Energy
$$\frac{\partial}{\partial t}(\rho E) = -\nabla \cdot \left(U(\rho E + p)\right) + k_{eff}\nabla^2 T \tag{4}$$

where k_{eff} is the effective conductivity and E is the total energy.

The local Nusselt number Nu (x,t) wherein the local wall heat transfer coefficient h is embedded, describes the convective heat transfer between the heated surface and the synthetic jet flow. Using orifice width d_o as the characteristic length, this is defined as,

$$Nu(x,t) = \frac{hd_o}{k_f} = \frac{\partial T}{\partial y}\frac{d_o}{\Delta T} \tag{5}$$

The Nusselt number is evaluated from the local surface normal temperature gradient, $\frac{\partial T}{\partial y}$ and the temperature difference $\Delta T = (T_w - T_b)$ where T_w is the local wall temperature and T_b is the average bulk fluid temperature the in the fluid domain.

2.3 Solution domain and boundary conditions

The 2-dimensional numerical simulation was formulated using the computational fluid dynamics software FLUENT. A structured mesh was used in the solution domain, as shown in Fig. 5 using GAMBIT mesh generation facility. The grid dependency of results was tested by observing the changes to the time-averaged velocity fields in the solution domain for varied grid sizes of 14000 (coarse), 48072 (medium) and 79000 (fine). In view of the moving mesh integrity and CPU time, the most appropriate grid size was found to be 48072 cells for a five percent tolerance between successive grid selections. In capturing intricate details of the jet formation and flow separation, the grid density in the vicinity of the orifice was refined to have 14 grid cells in the axial direction and 20 in the transverse direction.
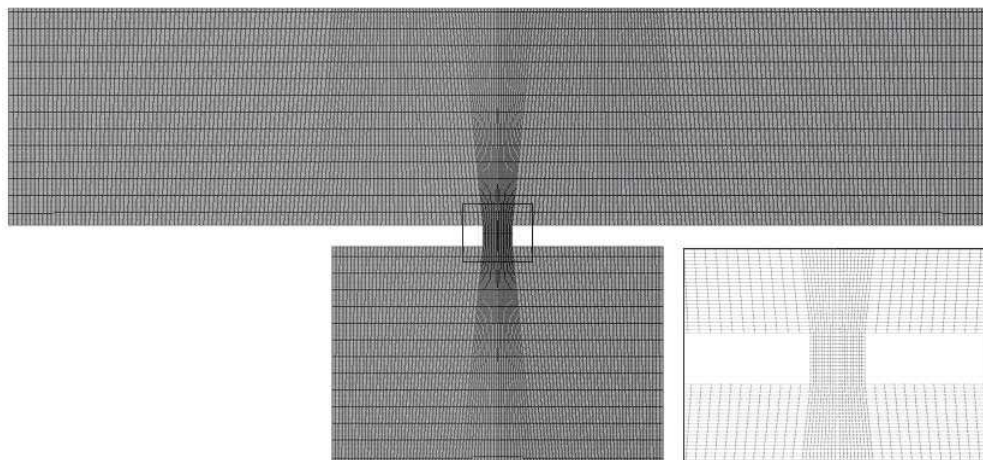

Fig. 5. Computational grid for solution domain (Inset shows enlarged view of the marked region)

Adiabatic conditions were applied at the cavity walls and the diaphragm while the heater surface was maintained at an isothermal temperature of 360 K. The (left) inlet to the heat sink flow passage was treated as a known constant velocity boundary while the (right) flow outlet was treated as pressure outlet boundary. It was assumed that the working fluid air is incompressible and has an inlet temperature of 300 K with constant thermodynamic properties under standard atmospheric conditions.

Arising from small geometrical length scales, synthetic jets generally tend to have small operating Reynolds numbers making flow turbulence seemingly unimportant. However, the oscillating nature of the flow may give rise to intense localised perturbations. In handling the wide flow variations, the Shear-Stress-Transport (SST) k-ω turbulence model was invoked in the model to provide an accurate representation of the near-wall region of wall-bounded turbulent flows. Initially, a 3 percent turbulence intensity was applied at the outlets, thereafter the flow was allowed to develop on its own through the inherent instabilities. The y+ and y* value in the wall region were found to be approximately 1, confirming that the near-wall mesh resolution is in the laminar sublayer.

2.4 Initial conditions and solution methodology

The initial (t = 0) position of the diaphragm was taken to be at the bottom of the cavity. A special User Defined Function (UDF) incorporating Dynamic-layering technique (FLUENT, 2004) was formulated and combined with the FLUENT solver to describe the periodic diaphragm movement. For this, the diaphragm displacement was expressed as y = A sin (ωt), where A is the diaphragm amplitude, ω is the angular frequency and t is time.

A segregated solution method with implicit solver formulation in FLUENT was used as the numerical algorithm while the Second-order discretisation schemes were employed for density, momentum, pressure, kinetic energy, specific dissipation rate and energy. The Pressure-Implicit with Splitting of Operators (PISO) scheme was used for pressure-velocity coupling. The bulk temperature of air at every time step was calculated using an UDF while the updated bulk temperature was fed back to the simulation for calculating local heat transfer coefficient and Nusselt number.

The jet Reynolds number (Re_c) was calculated based on the jet characteristic velocity U_c, which is defined by (Smith & Glezer, 1998) as,

$$U_c = L_s f = \frac{1}{T} \int_0^{T/2} u_0(t)\, dt \qquad (6)$$

where $u_o(t)$ is the jet velocity at the orifice discharge plane, ½T is the jet discharge time or half period of diaphragm motion, and L_s is the stroke length (defined as the discharged fluid length through orifice during the inward diaphragm stroke).

Considering the operating range given in Table 1, the unsteady, Reynolds-averaged Navier-Stokes equations and the energy equation were solved to obtain the simulated thermal behaviour of the synthetic jet hybrid heat sink. The simulation was carried out using 720 time steps per cycle wherein 20 sub-iterations were performed within each time step.

Parameter	Range
Heat sink inlet flow velocity, V_i (m/s)	0, 0.5, 1.0, 2.0
Diaphragm frequency, f (kHz)	10
Diaphragm Amplitude, A (μm)	0,25,50,75,100
Jet Reynolds Number, Re_c	15, 30, 46, 62
Distance from orifice to heated wall, H/d_o	10

Table 1. Parametric range for numerical simulation

At each time step of a cycle, the internal iterations were continued until the residuals of mass, momentum, turbulence parameters (k and ω) were reduced below 10^{-3} and energy residuals were reduced below 10^{-6}, which is the convergence criterion for the computation. Data were extracted at every twentieth time step giving 36 data points per cycle. It was observed that 10 diaphragm cycles would be sufficient to achieve quasi-steady operating conditions in this flow geometry. To increase accuracy, a 2D-double precision solver was used to solve the governing equations for heat and fluid flow.

3. Results and discussion

3.1 Model validation

The model validation for the present simulation was carried out by formulating a separate synthetic jet model to match the dimensions used in the published work of (Yao et al., 2006). These results were extensively incorporated in NASA Langley Research Centre Workshop (CFDVAL2004) in assessing the suitability of turbulence models for synthetic jet flows. The results of this workshop concluded that the Shear-Stress-Transport (SST) k-ω turbulence model works best among the URANS models for jet flows.

For validation, the predicted axial (y-velocity) was compared with the experimental jet velocities measured by (Yao et al., 2006) using the techniques of Particle Image Velocimetry (PIV), Hot wire anemometry and Laser Doppler Velocimetry (LDV). This comparison is shown in Fig. 6, where it is seen that the present simulation agreed very well with the experimental data validating the model and its accuracy.
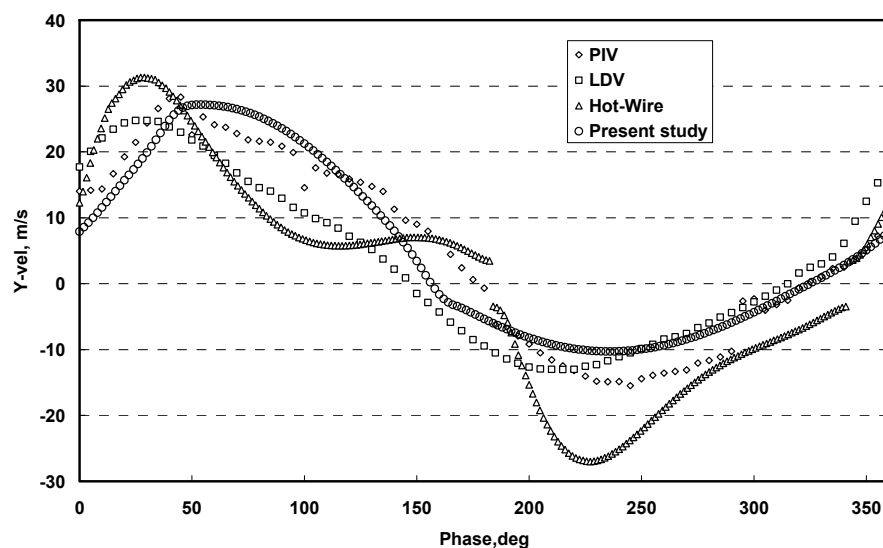
Fig. 6. Comparison of predicted axial/y-velocity of present work with the (PIV, LDV, Hot-wire) experimental data of (Yao et.al., 2006) at 0.1 mm from the orifice exit plane (f = 444.7 Hz, A=1.25 mm)

3.2 Velocity and fluid flow characteristics

For the synthetic jet operating frequency of 10 kHz and amplitude of 25 μm, Fig. 7 illustrates the diaphragm displacement and the jet discharge velocity over one cycle completed in 0.1 milliseconds. This jet velocity fluctuation resembles a sinusoidal pattern and verifies the net fluid mass discharge through the orifice to be zero for the synthetic jet operation.

Figs. 8 (a) and 8 (b) show typical time-lapsed velocity contours within the solution domain respectively for two separate cases of synthetic jet operation: (a) with stagnant fluid within heat sink (b) with flowing fluid in heat sink passages. It is seen that the simulation very well captures the intricate details of the synthetic jet discharge, subsequent vortex formation and the flow interaction between the jet and the cross-flow heat sink fluid stream.

During the diaphragm upward motion, a high-velocity fluid jet is discharged through the cavity orifice into the flow passage. Determined by diaphragm amplitude, sufficiently strong jet momentum enables the jet to penetrate the micro passage flow to reach the heated
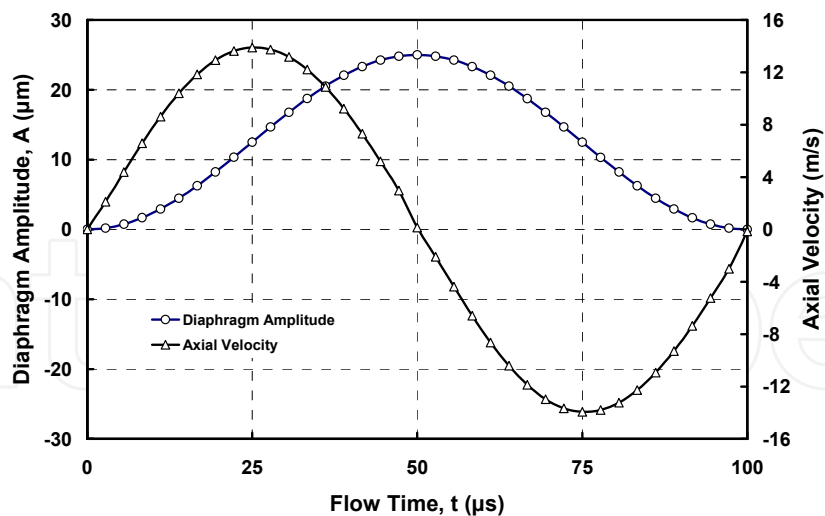
Fig. 7. Diaphragm displacement and jet velocity over one cycle at A = 25 μm and f = 10 kHz

(upper) wall within the time up to t = ½T at the peak diaphragm displacement. In the figures, the formation of synthetic jet vortices is clearly visible during this initial phase of sequence. The flow patterns exhibits symmetry in Fig. 8 (a) while the cross-flow drag imparted by the fluid stream in heat sink passage gives rise to asymmetry in Fig. 8 (b) where the jet is swayed in the streamwise direction. For t > ½T, the diaphragm retreats from its peak displacement to complete the cycle. During this final phase, the jet mechanism draws fluid back into the cavity. Meanwhile, already formed synthetic jet vortices are washed downstream by the fluid flow in heat sink passage.

Fig. 8(b) reveals that, even with the flow through heat sink, the synthetic jet still exhibits all of its fundamental characteristics corresponding to stagnant flow conditions. The synthetic jet periodically interrupts the flow through heat sink and breaks up the developing thermal and hydrodynamic boundary layers at the heated top wall. This cross-flow interaction creates steep velocity and temperature gradients at the heated surface as long as jet impingement occurs. This pulsating flow mechanism therefore leads to improved thermal characteristics in the synthetic jet-mounted heat sink.

The skewness in the jet discharge velocity profile is recognised as a prime factor in the process of synthetic jet vortex formation at the orifice. Fig. 9 shows the velocity vectors near jet orifice at t=T/2 (point of maximum jet expulsion) for two heat sink cross-flow velocities, V_i = 0.5 m/s and 2.0 m/s. The figure clearly indicates the existence of lateral flow velocities across the orifice mouth. This fluid motion induces fluid recirculation or entrainment within the orifice passage and its vicinity, encouraging the jet flow to diverge and form vortices. As illustrated, for higher heat sink cross-flow velocity, the fluid entrainment at the orifice becomes vigorous, hence producing stronger synthetic jet vortices.

The nature of synthetic jet movement through heat sink's cross flow is depicted in Fig. 10, where the axial jet velocity is plotted at several height elevations in the heat sink flow passage above the orifice plane. These velocity profiles are at t = T/2, where the diaphragm displacement is maximum with f = 10 kHz and A = 50 μm. The velocity profiles for a synthetic jet operating in stagnant fluid medium are also shown for comparison. These figures show that, the heat sink cross-flow drag shifts the point of impingement downstream of the flow passage with respect to jet operation in stagnant fluid. The jet impingement velocity is also somewhat attenuated with the increased cross-flow velocity.
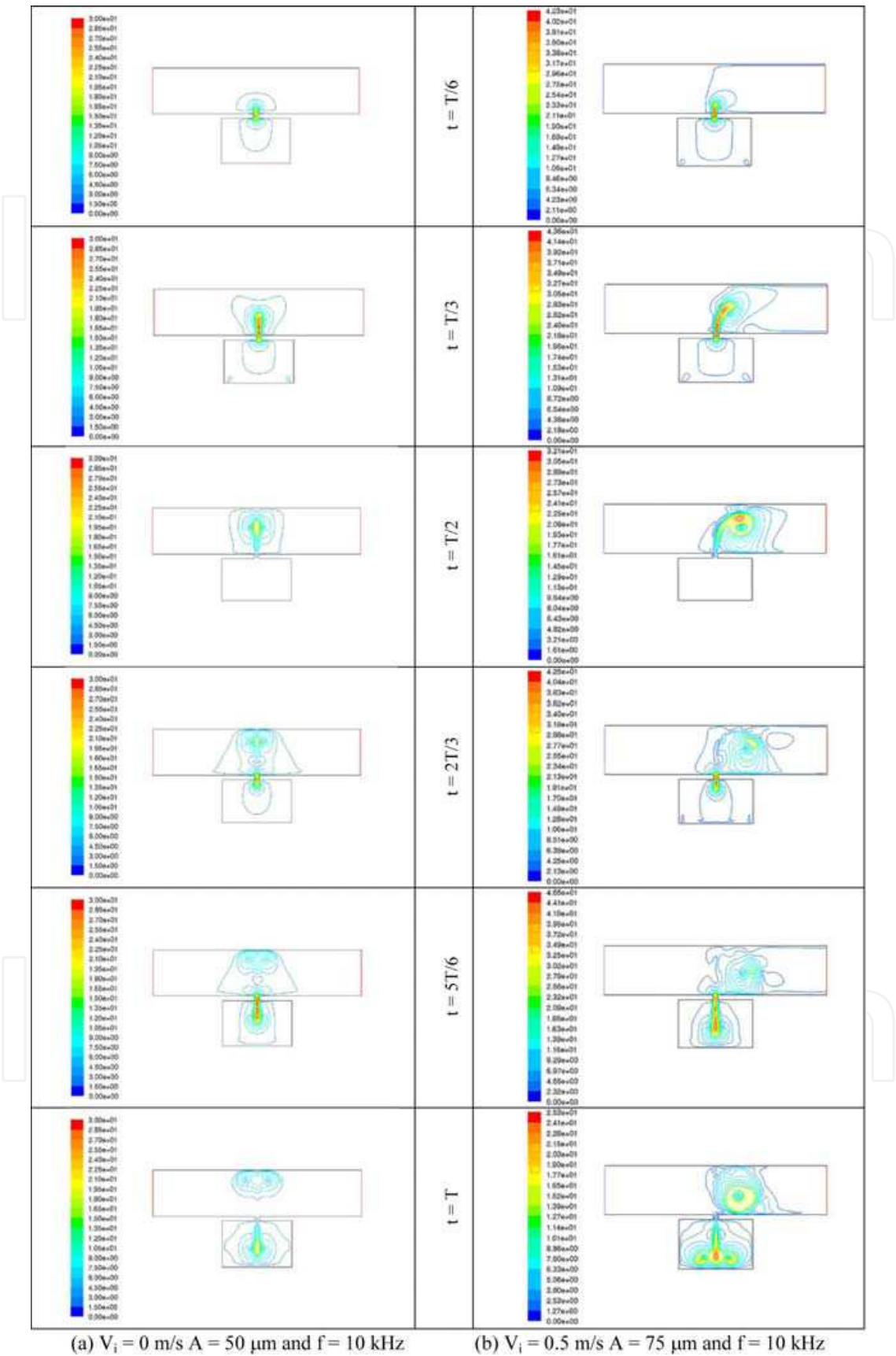
(a) $V_i = 0$ m/s $A = 50$ μm and $f = 10$ kHz   (b) $V_i = 0.5$ m/s $A = 75$ μm and $f = 10$ kHz

Fig. 8. Time-lapsed velocity contours over one diaphragm cycle
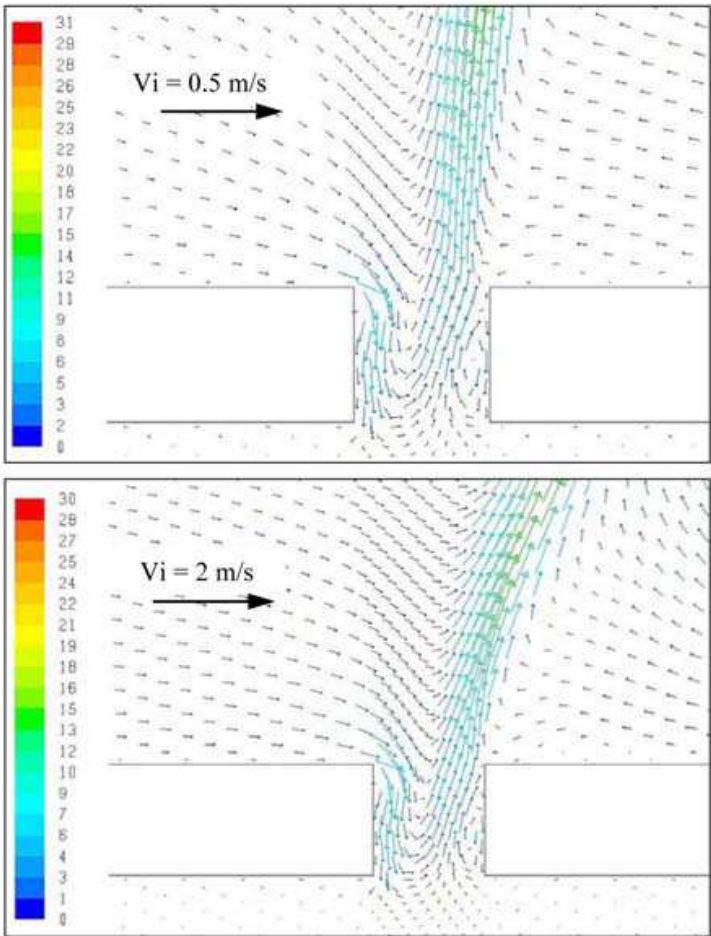
Fig. 9 Velocity vectors near the orifice at time t=T/2 (maximum expulsion)
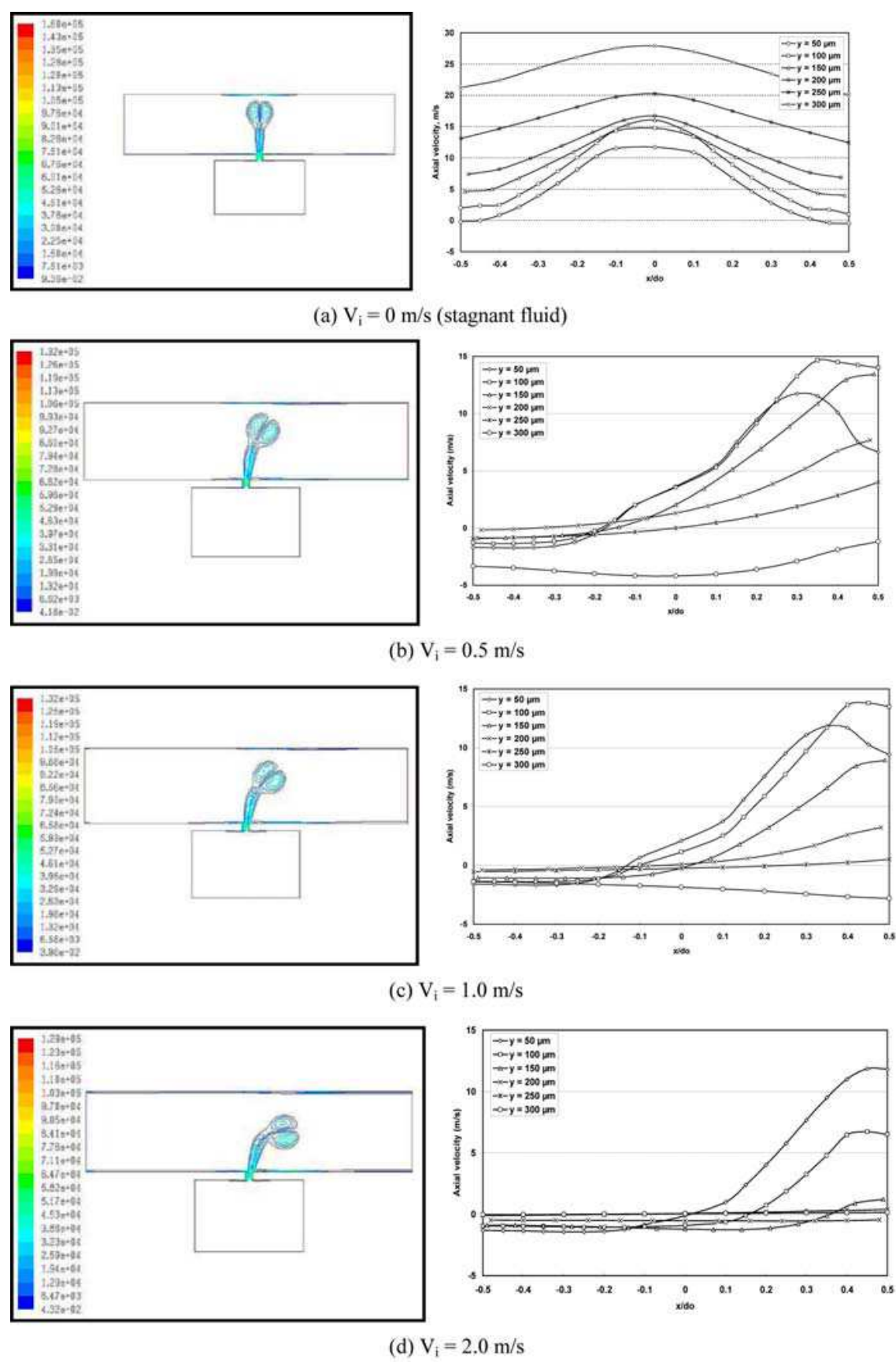f = 10 kHz, A = 50 μm *Note: Length of arrows and colours indicate velocity magnitude (m/s)*

(a) V_i = 0 m/s (stagnant fluid)

(b) V_i = 0.5 m/s

(c) V_i = 1.0 m/s

(d) V_i = 2.0 m/s

Fig. 10. Channel cross-flow effect on jet propagation at f = 10 kHz and A = 50 µm

(a) V_i = 0.5 m/s, f = 10 kHz　　　　　　(b) V_i = 1.0 m/s, f = 10 kHz
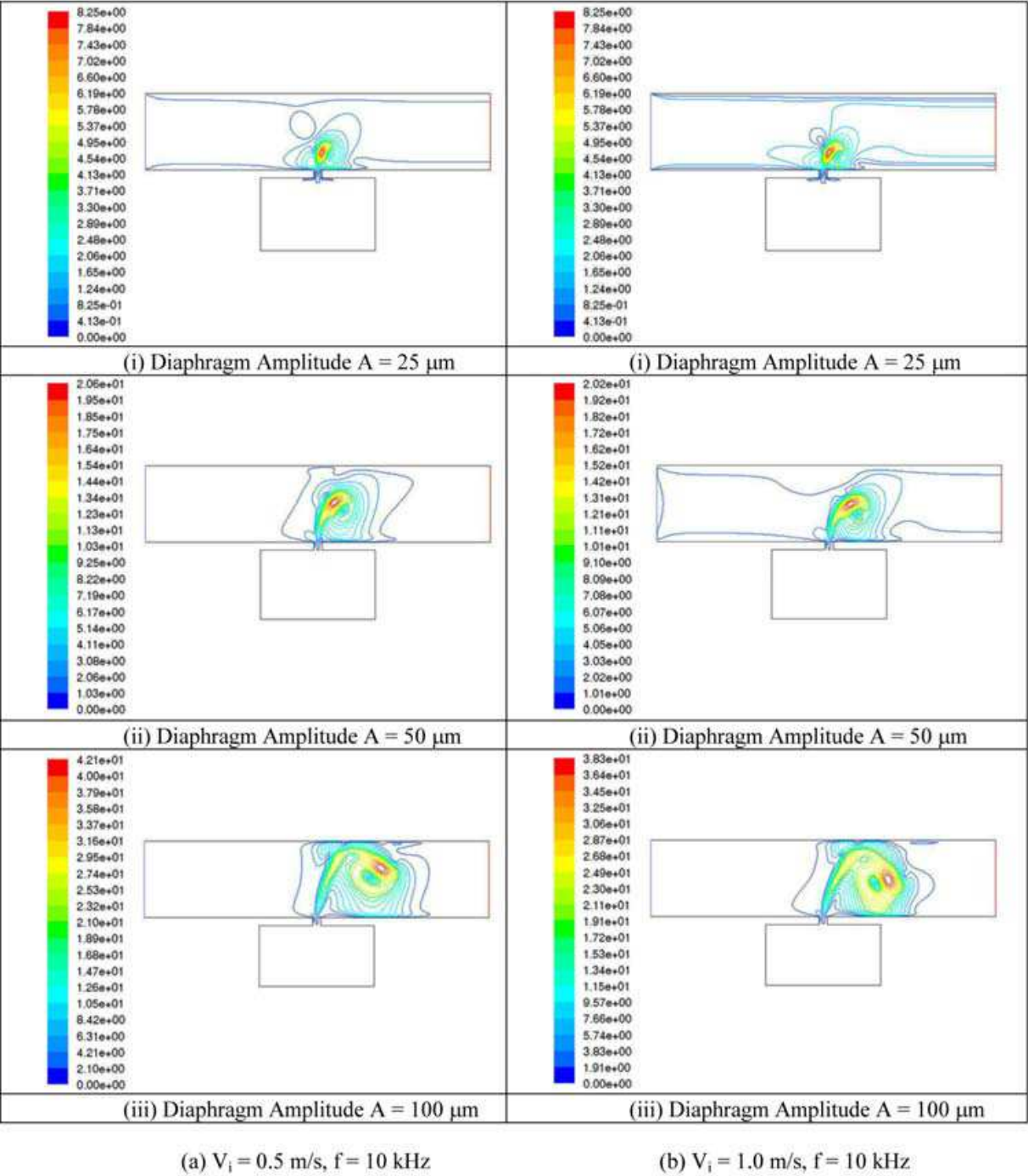
Fig. 11. Effect of diaphragm amplitude illustrated by velocity contours at t = ½ T

Relative strengths of the synthetic jet and the channel flow drag determine the extent of cross-flow interference and the boundary layer disruption at the heated wall. This is illustrated in Figs. 11(a) and 11(b) for heat sink flow velocities of 0.5 m/s and 1.0 m/s. It is clearly evident that the increased cross-flow causes the jet to be swayed downstream impeding the jet's penetrating ability through the boundary layer to reach the heated wall. Although this may reduce thermal benefits from jet impingement, the steeper velocity gradients generated by the cross-flow and jet interaction at the heated wall may improve forced convection heat transfer, leading to an increase in overall thermal performance.

3.3 Thermal characteristics and heat transfer enhancement

The vortex generation process of the synthetic jet creates fluid flow structures very conducive for heat transfer at the heated wall. This is effected by two major mechanisms: (a) development of steep temperature gradients at the heated wall due to periodic thinning of the thermal boundary layer arising from the synthetic jet and vortex impingement, and (b) vigorous mixing of heated fluid layers at the wall with the bulk fluid, thus rapidly transferring heat from the wall to the fluid. The temperature contours in Fig. 12 clearly illustrate these two mechanisms. It is seen that, the regions of high fluid temperature are essentially near the heated wall giving extremely high temperature gradients in that vicinity and, it takes only a few cycles for the temperature dispersion into the bulk fluid.

(a) After 1 cycle   (b) After 5 cycles

(c) After 10 cycles   (d) After 15 cycles

(e) After 20 cycles

300   320   340   360 (K)
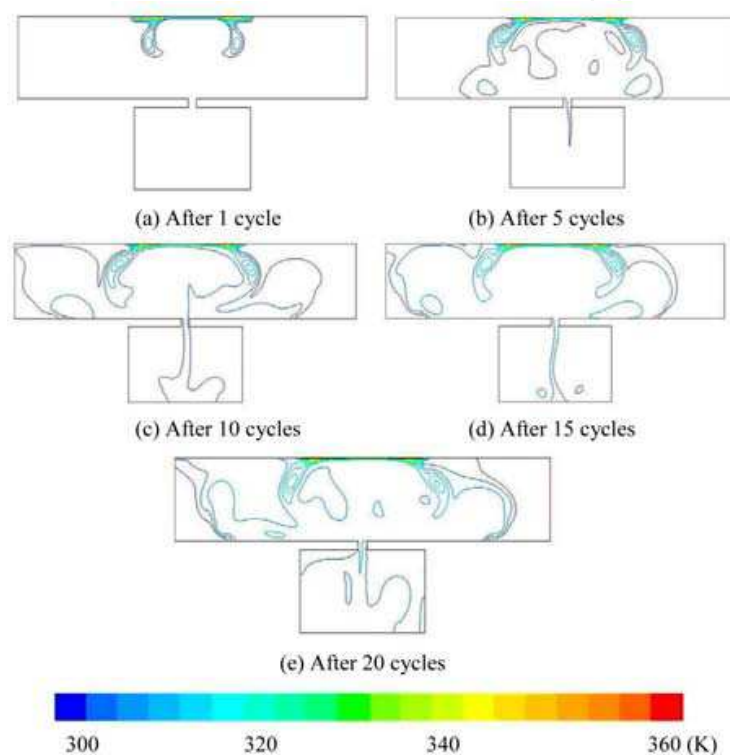
Fig. 12. Temperature contours within the solution domain after 1, 5, 10, 15 and 20 cycles

Over one diaphragm cycle, Figs. 13 and 14 show the distribution of local Nusselt numbers at the heated wall respectively, for the cases of with and without fluid flowing through the heat sink flow passage.

In Fig. 13 for $0 < t < \frac{1}{2}T$, the Nusselt number remains very low. This value is more or less similar to natural convection since the synthetic jet and vortices have yet to impinge on the heated surface. Nusselt number shows a very rapidly increase to about 23 when $t = 2T/3$, where the vortices begin to impinge on the heated surface. Subsequently, the Nusselt number gently declines for $t > 2T/3$ as the jet recedes and diaphragm descends. On the contrary, the variation of local Nusselt number in Fig. 14 shows a gentler rise over the entire heated wall during the cycle because of the forced convection due to the fluid flow in heat sink passage. At each time step, a peak is noticed in the distribution due to the jet and cross-flow fluid interaction. At $t = 2T/3$, the Nusselt number shows its highest value of about 13 in the cycle. The position of this peak is shifted downstream because of the cross-flow fluid drag swaying the impinging jet, as depicted in Figs. 8, 10 and 11.
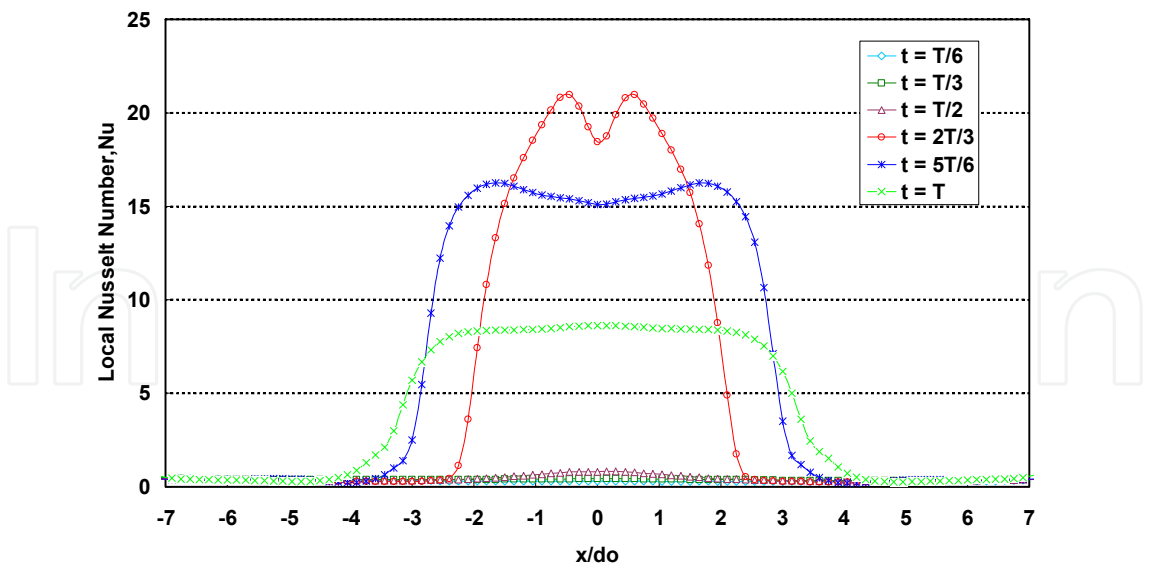
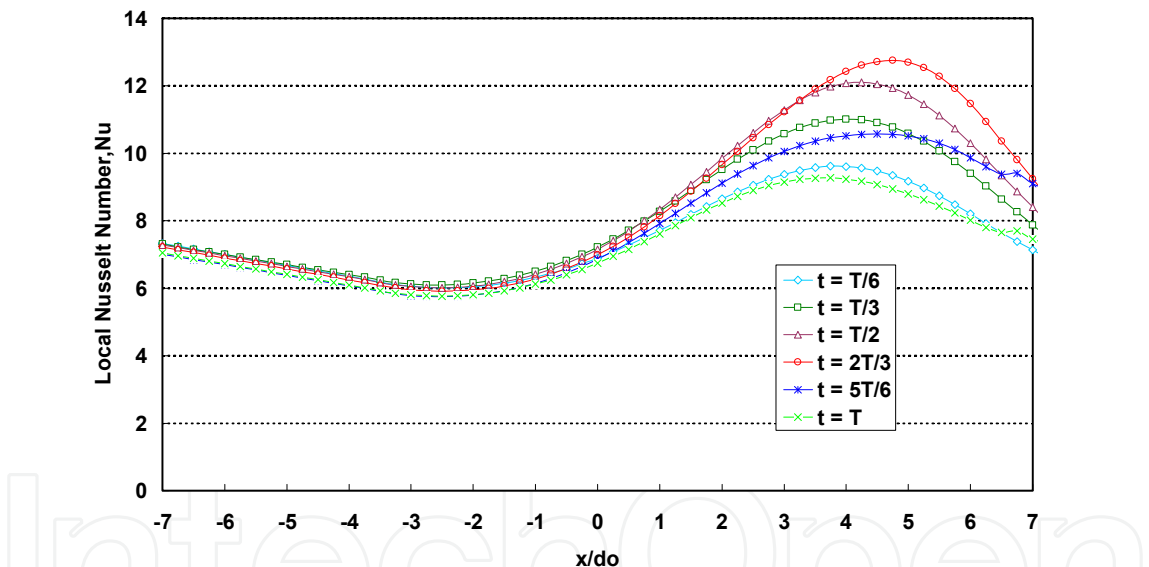Fig. 13. Local Nusselt number at heated wall with stagnant flow in heat sink over one cycle V_i =0 m/s, f = 10 kHz and A = 50 μm

Fig. 14. Local Nusselt number at heated wall with flowing fluid in heat sink over one cycle V_i =1 m/s , f = 10 kHz and A = 50 μm

In evaluating thermal benefits delivered by the synthetic jet interaction to heat sink passage, a separate simulation was performed without the diaphragm movement while retaining all the other geometrical and boundary conditions, as described before. For this pure forced convection heat sink without the synthetic jet, Fig. 15 shows the variation of local Nusselt number over the heated wall. It is observed that the Nusselt number asymptotically decays from the leading edge of heated wall with the developing flow. Taking this pure forced convection Nusselt number as the datum, the relative thermal performance of the hybrid synthetic jet-heat sink is evaluated and presented in Fig. 16, where the degree of thermal enhancement is expressed as the ratio of average heat sink Nusselt number with and

without synthetic jet operation. It is evident that, for the tested parametric range, the synthetic jet-based hybrid heat sink arrangement is capable of delivering up to 4.3 times (V_i=0.5 m/s) more heat transfer than an identical pure forced convection heat sink. Because of the nature of synthetic jet mechanism, this degree of thermal enhancement is realised without introducing additional net mass flow into the heat sink flow passage or needing additional fluid circuits. These are recognised as major operational benefits of this hybrid heat sink mechanism. Fig. 16 further shows that, higher cross-flow velocity impairs thermal enhancement. This is a manifestation of channel flow drag swaying the synthetic jet downstream preventing jet impingement. As the jet Reynolds number (or jet velocity or diaphragm amplitude) is increased for a given cross-flow velocity, the thermal enhancement rapidly increases when the jet is able to penetrate and reach the heated surface.
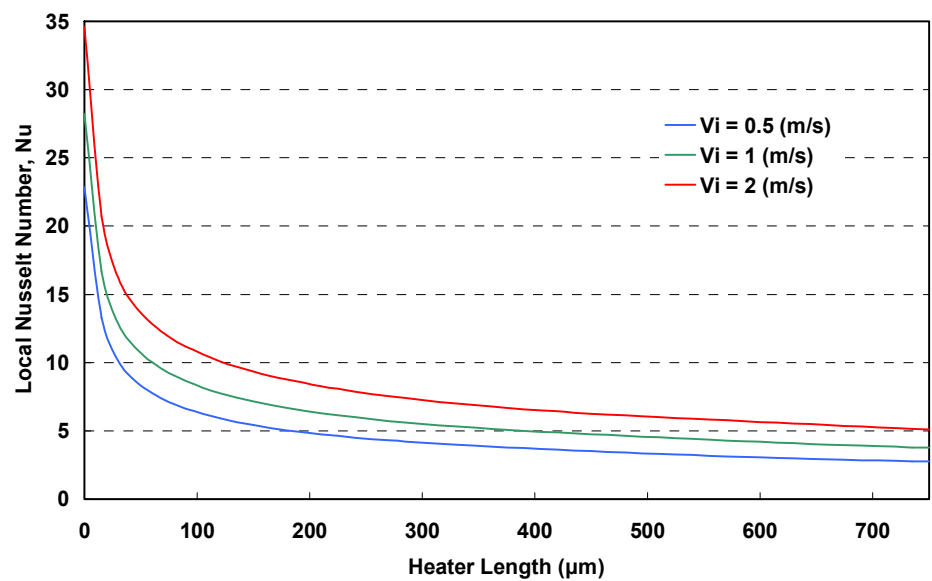
Fig. 15. Variation of Nusselt number along the heater surface without synthetic jet
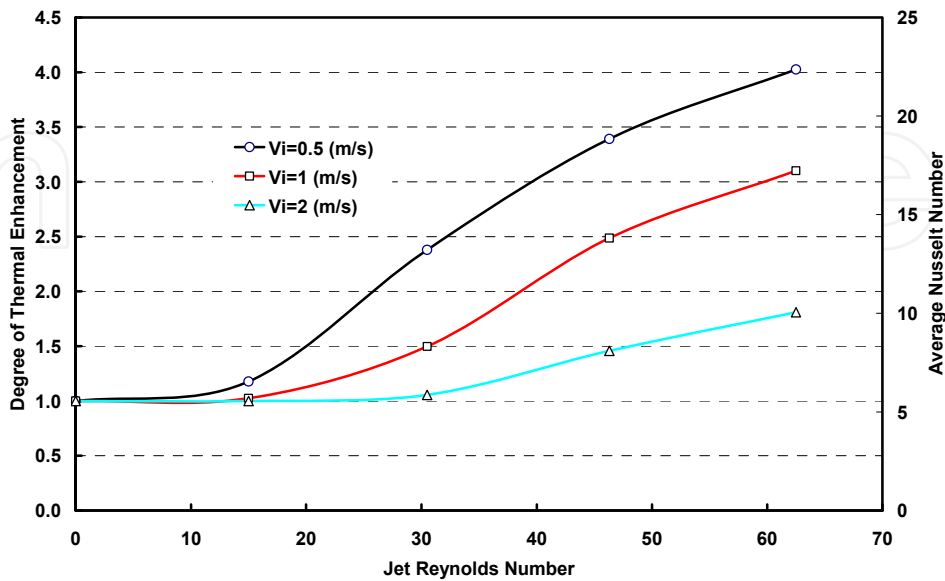
Fig. 16. Degree of thermal enhancement in heat sink due to synthetic jet mechanism

For increasing channel velocity, Fig. 17 shows the thermal performance and pressure drop of a heat sink without synthetic jet mechanism. If this heat sink were to deliver, for example, 4.3 times thermal enhancement, it would require a 40-fold high velocity from a datum value of 0.5 m/s. This would result in 70 times more channel pressure drop. On the other hand, the synthetic jet-based hybrid heat sink achieves 4.3-fold thermal enhancement with 0.5 m/s channel flow velocity with no increase in pressure drop. This clearly signifies the thermal enhancement potential of this hybrid arrangement and its operational benefits.
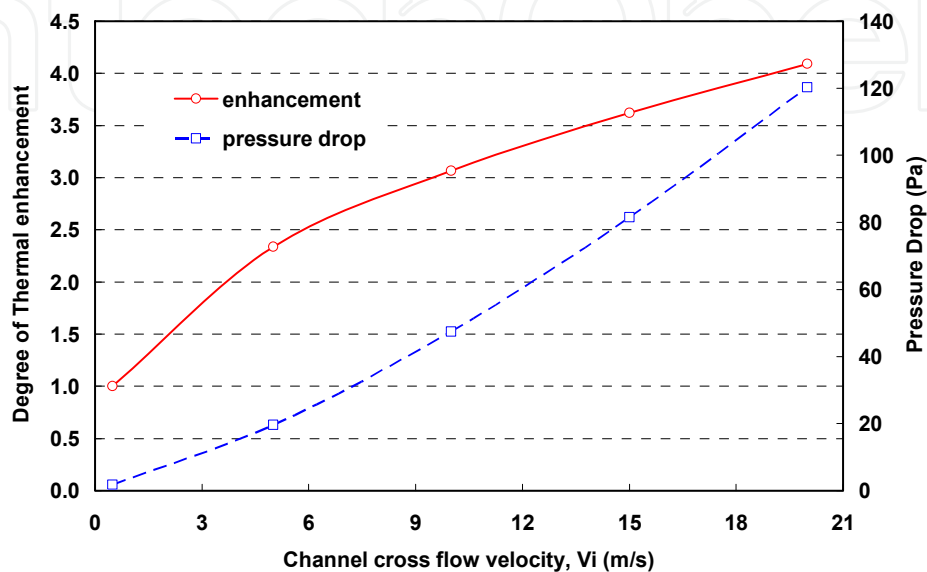
Fig. 17. Degree of thermal enhancement and pressure drop without synthetic jet mechanism

3.4 Fluid compressibility effects on synthetic jet performance

The compressibility of air mass within the cavity may affect the jet discharge, thus the heat sink performance, when the diaphragm operating frequency is varied. In examining this, two identical simulations are carried out and the results are compared. The first case is performed assuming constant air density, so that the fluid compressibility is totally eliminated. In the second case, the fluid density is taken to be dependant on local pressure in the solution domain with all the other simulation parameters being identical.

For the analyses with and without air compressibility, Fig. 18 illustrates the variation of Nusselt number with diaphragm frequency. The Nusselt numbers for both cases closely follow each other and increase almost linearly up to about 20 kHz. Beyond this, the Nusselt number predicted by the compressibility analysis quickly deviates and indicates a drop in magnitude while the incompressible Nusselt number continues to grow. The former behaviour shows a minimum at a frequency of around 80 kHz in heat sink with stagnant channel flow. At this frequency, the fluid discharge through the orifice is observed to cease. This is attributed to the simultaneous expulsion and ingestion of air neutralising the flow though the orifice or formation of standing waves. Therefore, a temporary breakdown occurs in the synthetic jet thermal effectiveness. However, the performance readily recovers beyond this critical diaphragm frequency. When the cross-flow is introduced, this limiting frequency is dramatically reduced to about 40 kHz at 0.5 m/s channel velocity. It is thought to be due to choking of the orifice arising from the increased flow entrainment at the orifice passage, as previously explained with respect to Fig. 9.
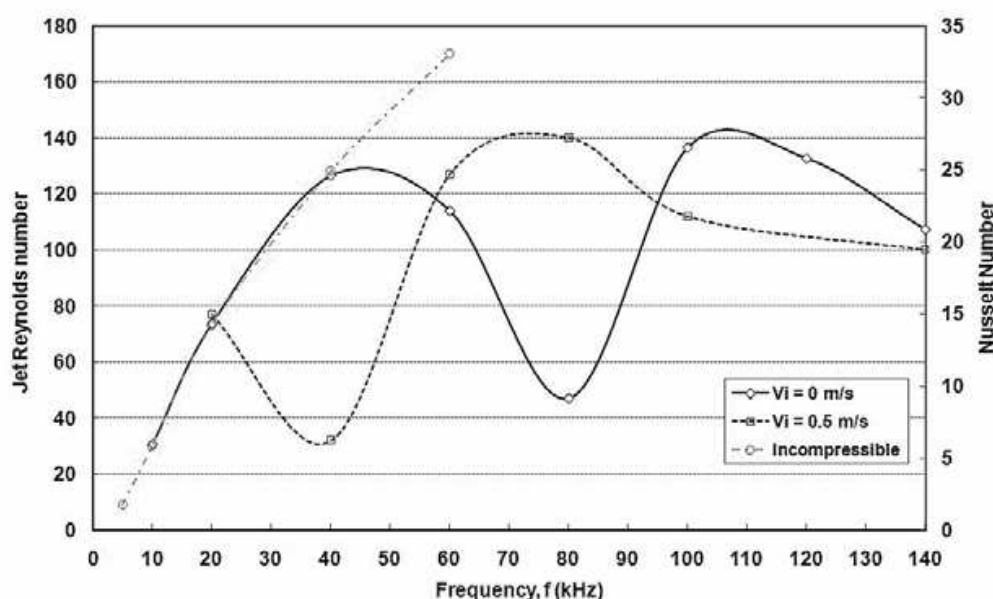
Fig. 18. Effect of compressibility on synthetic jet heat sink characteristics

4. Conclusions

This study has successfully demonstrated a novel technique for enhancing thermal performance of pure convective heat sinks in electronic cooling applications. The proposed method utilises a periodic fluid jet called "Synthetic Jet" that is injected into the heat sink's flow channel with a large fluid momentum but with zero averaged fluid mass discharge. The interaction between the jet and the fluid flow in channel creates excellent thermal characteristics at the heated wall thereby enhancing the heat sink's thermal performance. In the tested range, this synthetic jet-based heat sink delivers up to 4.3 times more wall heat transfer compared to an identical pure convection heat sink. Under incompressibility conditions, the thermal performance continues to grow with the increased diaphragm frequency. When the fluid compressibility is accounted for, the thermal performance temporarily falls upon reaching a certain frequency and then recovers with further frequency increase. This hybrid flow system has a unique ability to achieve excellent heat transfer rates without higher channel flow velocities in heat sink or causing pressure drop increases in flow passage. Also, this mechanism does not require additional fluid circuits to achieve such high heat transfer rates. These are identified as key operational attributes that set it apart from other thermal enhancement strategies.

5. References

Chu, R C. (2003). The Perpetual Challenges of Electronic Cooling Technology for Computer Product Applications-from laptop to supercomputers. *National Taiwan University Presentation*, November 12, 2003, Taipei, Taiwan.

Campbell, J S.; Black, W Z. & Glezer, A. (1998). Thermal Management of a laptop Computer with Synthetic Air Microjets, *InterSociety Conference on Thermal Phenomena, IEEE*, 43-50.

Erbas, N. & Baysal, O. (2009). Micron-level actuators for thermal management of microelectronic devices, *Heat Transfer Engineering*, Vol. 30, No. 1-2, 138-147.

FLUENT User Guide Manual 6.2.16, 2004.

Gillespie, M B.; Black, W Z.; Rinehart, C. & Glezer, A. (2006). Local Convective Heat Transfer From a Constant Heat Flux Flat Plate Cooled by Synthetic Air Jets, *Journal of Heat Transfer*, Vol. 128, 990-1000.

Go, D B. & Mongia, R K. (2008). Experimental studies on synthetic jet cooling enhancement for portable platforms. *IEEE*, 528-536.

Holman, R.; Utturkar, Y.; Mittal, R; Smith, B L. & Cattafesta, L. (2005). Formation criterion for synthetic jets. *AIAA Journal*, Vol. 43, No. 10, 2110-2116.

Lee, P S.; Garimella, S V. & Liu, D. (2005). Investigation of Heat Transfer in Rectangular Microchannels, *International Journal of Heat and Mass Transfer*, Vol. 48, No. 9, 1688-1704.

Lee, P S. & Garimella, S V. (2006). Thermally Developing Flow and Heat Transfer in Rectangular Mircochannels, *International Journal of Heat and Mass Transfer*, Vol. 49, No. 17, 3060-3067.

Mahalingam, R. & Rumigny, N. (2004). Thermal Management using synthetic jet ejectors. *IEEE,* Vol. 27, No. 3, 439-444.

Narayanaswamy, R.; Chandratilleke, T.T & Foong, J L. (2008). Laminar convective heat transfer in a microchannel with internal fins. *Proceedings of the 6th International ASME Conference on Nanochannels, Microchannels and Minichannels*, (ICNMM 2008-62044), Darmstadt, Germany.

Palm, B. (2001). Heat Transfer in Microchannels. *Microscale Thermophysical Engineering*, Vol. 5, 133-175.

Pavlova, A. & Amitay, M. (2006). Electronic Cooling Using Synthetic Jet Impingement, *Journal of Heat Transfer*, Vol. 128, No. 9, 897-907.

Qu, W. & Mudawar, I. (2002). Experimental and Numerical Study of Pressure Drop and Heat Transfer in a Single Phase Microchannel Heat Sink, *International Journal of Heat and Mass Transfer*, Vol. 45, No. 2, 2549-2565.

Steinke, M E. & Kandlikar, S G. (2004). Single Phase Heat Transfer Enhancement Technique in Microchannel and Minichannel Flows, *International conference of Microchannel and Minichannels*, ICMM 2004-2328, 141-148.

Smith, B L. & Glezer, A. (1998). The formation and evolution of synthetic jets. *Physics of fluids*, Vol. 10, No. 9, 2281-2297.

Timchenko, V.; Reizes, J. & Leonardi, E. (2004). A numerical study of enhanced micro-channel cooling using a synthetic jet actuator. *Proceedings of the 15th Australasian Fluid Mechanics Conference,* Sydney, Australia.

Utturkar, Y.; Arik, M. & Gursoy, M. (2007). Assessment of cooling enhancement of synthetic jet in conjunction with forced convection, *Proceedings of IMECE2007,* November 11-15, Seattle, USA.

Yao, C S.; Chen, F J. & Neuhart, D. (2006). Synthetic Jet Flowfeild Database for Computational Fluid Dynamics Validation, *AIAA*, Vol. 44, No. 12, 3153-3157.
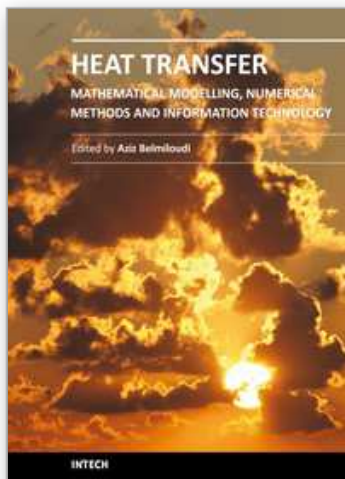
Heat Transfer - Mathematical Modelling, Numerical Methods and Information Technology
Edited by Prof. Aziz Belmiloudi

Over the past few decades there has been a prolific increase in research and development in area of heat transfer, heat exchangers and their associated technologies. This book is a collection of current research in the above mentioned areas and describes modelling, numerical methods, simulation and information technology with modern ideas and methods to analyse and enhance heat transfer for single and multiphase systems. The topics considered include various basic concepts of heat transfer, the fundamental modes of heat transfer (namely conduction, convection and radiation), thermophysical properties, computational methodologies, control, stabilization and optimization problems, condensation, boiling and freezing, with many real-world problems and important modern applications. The book is divided in four sections : "Inverse, Stabilization and Optimization Problems", "Numerical Methods and Calculations", "Heat Transfer in Mini/Micro Systems", "Energy Transfer and Solid Materials", and each section discusses various issues, methods and applications in accordance with the subjects. The combination of fundamental approach with many important practical applications of current interest will make this book of interest to researchers, scientists, engineers and graduate students in many disciplines, who make use of mathematical modelling, inverse problems, implementation of recently developed numerical methods in this multidisciplinary field as well as to experimental and theoretical researchers in the field of heat and mass transfer.

INTECH
open science | open minds

www.intechopen.com

Fax: +385 (51) 686 166
www.intechopen.com

Fax: +86-21-62489821